



HAL
open science

Multi-Physical Model for Sizing Optimization of Electrical Machines

Wissem Bekir, Oualid Messal, Louis Lambourg, Frédéric Dubas, Souad Harmand, Afef Kedous-Lebouc, Frédéric Gillon

► **To cite this version:**

Wissem Bekir, Oualid Messal, Louis Lambourg, Frédéric Dubas, Souad Harmand, et al.. Multi-Physical Model for Sizing Optimization of Electrical Machines. Conference on Electromagnetic Field Computation, Nov 2020, Pisa, Italy. hal-03053044v1

HAL Id: hal-03053044

<https://hal.science/hal-03053044v1>

Submitted on 10 Dec 2020 (v1), last revised 3 May 2021 (v2)

HAL is a multi-disciplinary open access archive for the deposit and dissemination of scientific research documents, whether they are published or not. The documents may come from teaching and research institutions in France or abroad, or from public or private research centers.

L'archive ouverte pluridisciplinaire **HAL**, est destinée au dépôt et à la diffusion de documents scientifiques de niveau recherche, publiés ou non, émanant des établissements d'enseignement et de recherche français ou étrangers, des laboratoires publics ou privés.

Multi-Physical Model for Sizing Optimization of Electrical Machines

W. Bekir¹, O. Messal¹, L. Lambourg², F. Dubas³, S. Harmand², A. Lebouc⁴, and F. Gillon¹

¹ Univ. Lille, Arts et Metiers Institute of Technology, Centrale Lille, Yncrea Hauts-de-France, ULR 2679- L2EP, F-59000 Lille, France.

² University of Valenciennes, LAMIH, CNRS UMR 8201, Campus le Mont Houy, Valenciennes F59313.

³ Département ENERGIE, FEMTO-ST, CNRS, Univ. Bourgogne Franche-Comté, F90000 Belfort, France.

⁴ Univ. Grenoble Alpes, CNRS, Grenoble INP, G2Elab, F38000 Grenoble, France.
 wissem.bekir@centralelille.fr, frederic.gillon@centralelille.fr

This paper presents a layered multi-physical model for sizing optimization as well as solving a specific optimization problem of interior permanent-magnet (PM) synchronous machine (IPMSM) for traction application. The advantages of the model structure are the management of the calculation time and the multi-physical aspect taking into consideration the iron losses and the thermal phenomena. An analysis is conducted over an optimization problem with different nested loops and for several operating points of the IPMSM.

Index Terms—Electrical machines, electric traction vehicle, multi-physical model, sizing optimization.

I. INTRODUCTION

To enable the ecological transition toward cleaner and greener transportation, the automotive manufacturers partially or totally electrify their new models. The electrical machine is one of the key elements of the electrical traction chain which considerably affects the vehicle performances and the energetic efficiency. A traction machine should be able to reach the desired technical performances while having minimal losses over the whole operating cycle [1]. In this framework, the optimal design of the electrical machines is of prime importance for the electrical vehicle (EV) manufacturers. The electric machine design is a complex process requiring the use of a dedicated design model. The latter has to be sufficiently fast because it is intended to be run repeatedly by an optimization process to reach the optimal solution regarding the imposed constraints. In addition, the design model has to take into consideration all the essential phenomena for a realistic evaluation of the desired performances.

Some studies on the electric machine optimization field exist. In [2], finite-element analysis (FEA) based optimal design of an IPMSM has been considered. In this study, only the magnetic behavior has been studied with the aim of reducing the torque ripple and a total harmonic distortion. Although the thermal phenomena and the iron losses within the machine have not been considered, the authors point out the problem of the numerical computation time with the developed optimization tool. In [3], a magnetic loss model is coupled to a 2D FEA of a wound rotor synchronous machine. The control optimization of the studied machine has been achieved by considering the total losses (Joule and iron losses) instead of the classical approaches that consider only the Joule losses. This work shows the difficulty to optimize the control of the studied machine as well as the importance of taking into account the iron losses in the optimization procedure. Nevertheless, the sizing parameters have not been studied and the impact of the machine thermal behavior has been neglected.

In [4], an optimization design of a switched reluctance machine (SRM) with a layered multi-physical semi-analytical model has been studied. The model based on the magnetic equivalent circuit (MEC) is used to solve the electromagnetic

field and coupled to simple iron loss and thermal models. Although the used models are relatively simple, the proposed approach is particularly relevant for the SRM application.

In the present study, a layered multi-physical semi-analytical model intended to optimize a traction IPMSM has been developed. The model is designed to be modular. It is built in such a way that different granularities are offered to the designer in order to adjust the compromise between efficiency and accuracy. The whole physical phenomena involved in the application are considered based on three advanced models developed by specialists of each physics and coupled to form a consistent model dedicated to the design of a traction system.

The paper is organized as follows: Section II underlines the multi-physical model coupling structuration with its different layers as well as the calculation time of each sub-model corresponding to each physics. In section III, a problem of traction machine design has been formulated as an optimization problem and solved for different operating points. Temperature, control and geometry loops have been considered. Finally, in section IV, the results are presented and analyzed. The selected example shows the difficulties lying behind the resolution of a multi-physical problem in a system context.

II. MULTI-PHYSICAL MODEL FOR SIZING OPTIMIZATION

A. Description

The multi-physical machine design model has been established by coupling three advanced models as shown in Fig.1. The first layer contains a generalized nonlinear adaptive MEC (or bidirectional reluctance network). It incorporates the saturation effect and uses the air-gap sliding-line technic to connect the static part (stator) and the moving part (rotor) of the machine. A detailed description of the model and the non-linear system resolution is given in [5]. The second layer contains three iron loss models with different accuracy levels (high, medium and coarse) [6]-[8]. The most accurate loss model used is the so-called loss surface (LS) model [8] that evaluates the iron losses in the machine based on the magnetic flux density waveforms given by the MEC. The third layer contains a 3-D aero-thermal model baptized SAME. This model allows

determining the thermal machine behavior depending on different aero-thermal conditions related to the cooling system and to the machine motion. SAME is nodal-based model which consists in discretizing the machine geometry into several isothermal volumes wherein the centers are connected by thermal conductances [9]. The temperature field is calculated in each zone of the machine knowing the power loss distribution (Joule losses P_{Joule} calculated by MEC and iron losses P_{Iron} determined by the iron loss model).

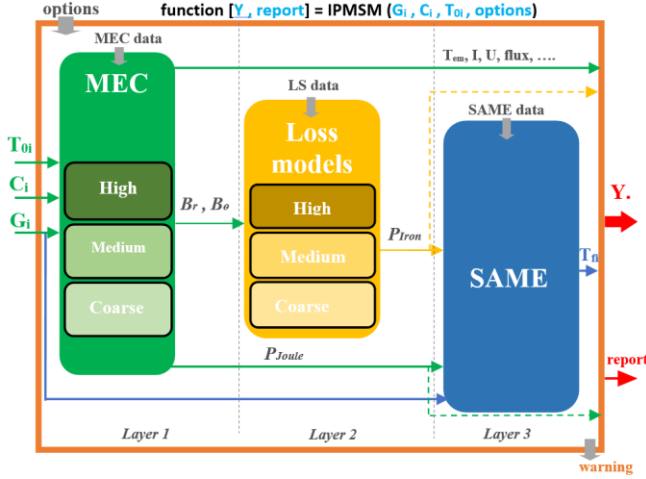


Fig. 1. Block diagram of the sizing model with different discretization levels (high, medium or coarse) allowing a compromise between accuracy and computation time.

This sizing model is structured as an only Matlab® function named IPMSM with input and output data. The inputs are the geometrical parameters of the machine G_i , the control parameters C_i , the initial temperatures T_{0i} and the options as the choice of the MEC discretization type, the choice of the iron loss model and the coupling between layers: (1, 1-2, or 1-2-3). Some options allow handling other functionalities like the parallel calculation used for the iron loss model, displaying the calculation progress graph, etc.

The IPMSM model has 16 geometric variables G_i , 2 control variables C_i and 3 initial temperatures T_{0i} . Their outputs are in the form of temporal vectors or space matrix. The quantities are both local (e.g., flux density in each magnetic element of the machine) and global (e.g., the losses of the winding heads or the PM temperatures). Such structuration is necessary to implement an adaptive design process.

B. Computation Time

The total execution time of the multi-physical model depends on the desired accuracy level. The MEC spatial discretization affects the iron loss model calculation times. Table I represents the calculation times for the different coupling layers executed on a classical computer (Intel® Core™ i7-6700 CPU @ 2.6 GHz RAM 8 Go 64 bits); the idea is to see the order of magnitude of calculation time for each layer. The MEC calculation time for the medium level is a less than 9 s. Nevertheless, if we need to use the high precision iron loss model, even with the coarse MEC, the calculation time becomes more important (around 60 s). Notice that the SAME computation time is of around 1 ms.

Table I. Calculation times for each layer of the sizing model.

		Computing time [s]				SAME
		MEC	Loss models			
			High	Medium	Coarse	
MEC	High	38.0	578	0.17	0.0069	0.0012
	Medium	8.5	72	0.12	0.0036	
	Coarse	3.8	56	0.1	0.003	

III. OPTIMIZATION PROBLEM

As mentioned before, the purpose is to design an IPMSM dedicated to an EV traction application. The problem is typical; the machine should be able to reach predefined torque-speed operating points though with the minimum of losses and without abusively exceeding critical temperatures. Fig.2 shows eight operating points distributed over the torque-speed plane. Each point is characterized by a torque value T_{emj} , a speed value Ω_j and weight called w_j represented in the figure by the dots size. This weight has been chosen according to technical specifications.

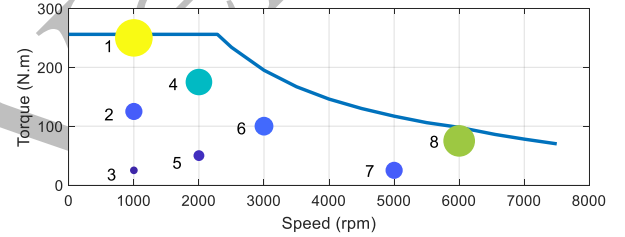


Fig. 2. Operating points with different weights distributed over the torque-speed plane.

The optimization problem is described by three nested loops of the equation system (1). The O1 loop allows identifying the temperatures vector of the machine T_0 . The control loop O2 allows the two parameters of the control necessary to reach the desired torque T_{emrefj} for a given speed Ω_{refj} to be identified for each operating point ((the control angle ψ and the stator current amplitude I_s). This is performed while minimizing the total power losses and without exceeding the voltage and the maximal current thresholds V_{RMSMax} and I_{smax} at the power electronic converter output.

$$\begin{aligned}
 & \text{O3} \left[\min_{(L_s, N_s)} \left(\frac{1}{n_{pts}} \sum_{j=1}^{n_{pts}} w_j (P_{Joule} + P_{Iron}) \right) \right. \\
 & \quad \text{O2} \left[\min_{(w_j, I_{sj})} (P_{Joule} + P_{Iron}) \text{ for } j = 1 : n_{pts} \right. \\
 & \quad \quad \text{O1} \left[\min_{T_{0j}} \|T_{fj} - T_{0j}\| \right. \\
 & \quad \quad \psi_{\min} \leq \psi_j \leq \psi_{\max} \\
 & \quad \quad I_{s\min} \leq I_{sj} \leq I_{s\max} \\
 & \quad \quad V_{RMSj} - V_{RMSMax} \leq 0 \\
 & \quad \quad T_{emrefj} - T_{emj} \leq 0 \text{ with: } \Omega_j = \Omega_{refj} \\
 & \quad \quad L_{s\min} \leq L_s \leq L_{s\max} \\
 & \quad \quad N_{s\min} \leq N_s \leq N_{s\max}
 \end{aligned} \tag{1}$$

Finally, the third loop O3 enables optimizing two design parameters: the stator length L_s , and the turn number N_s of the stator phases. The objective function of the O3 loop is formulated as a function of the power losses sum and the weight of the n_{pts} operating points (see Fig.2).

A. Temperature loop – O1

This loop allows identifying the temperatures of different parts of the machine for steady state operation. The model takes as input the initial temperatures of the active winding part $T_0(1)$, the winding heads $T_0(2)$ and the PMs $T_0(3)$. To evaluate the steady state final temperatures, an iterative process was added allowing minimizing the difference between the final and the initial temperatures. The convergence criterion ε for the iteration k , is defined as follows :

$$\varepsilon = \frac{\|T_{fk} - T_{0k}\|}{\|T_{fk}\|} < tol \quad (2)$$

Fig. 3 shows the convergence criterion evolution for the operating point 250 A @ 1,000 rpm on a log scale for different initial vectors of temperature. The number of iterations needed to obtain convergence is relatively low (5 iterations $\cong \varepsilon < 10^{-2}$).

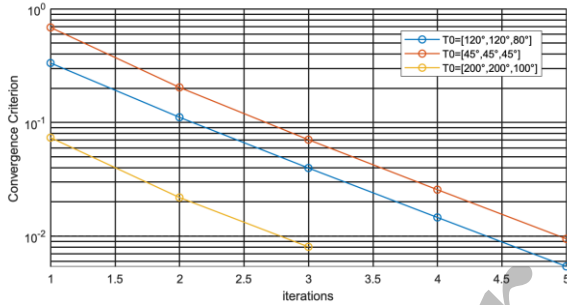


Fig. 3. Convergence criterion evolution for the operating point 250 A @ 1,000 rpm.

B. Control loop – O2

The weakening regime is managed by the control loop to respect the constraints on torque, voltage and current. All the magnetic phenomena taken into consideration in the IPMSM model are used to find control variables ψ and I_s .

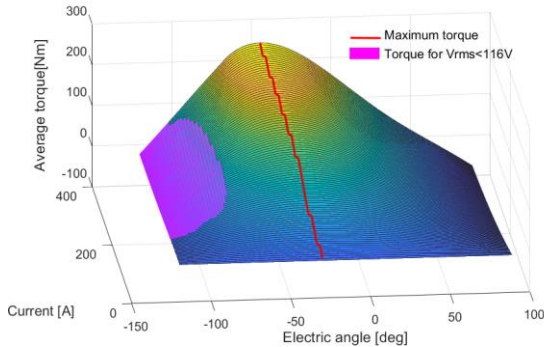


Fig. 4. Evolution of the torque as a function of electric angle ψ and current I_s for a rotation speed of 5,000 rpm.

If this optimization does not converge, it means that the operating point is unachievable for the defined machine. Following this approach, the robustness of the control loop is very important. Fig.4 shows the torque evolution as a function

of ψ and I_s for a rotation speed of 5,000 rpm. The red line represents the progress of the maximal achievable torque without the voltage constraint. The purple area shows the achievable torque for a voltage constraint $V_{RMSMax}=116$ V. The areas are quite smooth, an optimization method based on gradient could be chosen. The identification of a control takes around 30 evaluations of the model.

C. Geometry loop – O3

Two geometrical parameters (the machine length L_s and the number of winding turns N_s) are selected to provide a typical case study and test the sizing process.

IV. RESULTS AND ANALYSIS

To assess the thermal loop effect on the machine behavior and performances, the study has been conducted in two parts. The optimization problem is first solved for an initial fixed temperature and then the thermal loop O1 was added.

A. Without the temperature loop

Fig.5 illustrates the (L_s, N_s) achievable areas for four selected operating points: no.1, 4, 6 and 8, indicated in Fig.2 and the associated winding temperature evolution. The studied area is: $L_s = [60, 100] \times 10^{-3}$ m and $N_s = [28, 50]$. The figure shows that the achievable domain is reduced in an opposite way in the case of the operating point 1 (low speed and high torque) and the point no. 8 (high speed and low torque). The winding temperature is highly affected by L_s in the case of the operating point no.1 and by the number of winding turns N_s in the case of the operating point no.8. The operating point no. 6 is set in weakening state wherein a valley appears clearly. Notice that all the model output quantities can be plotted and analyzed.

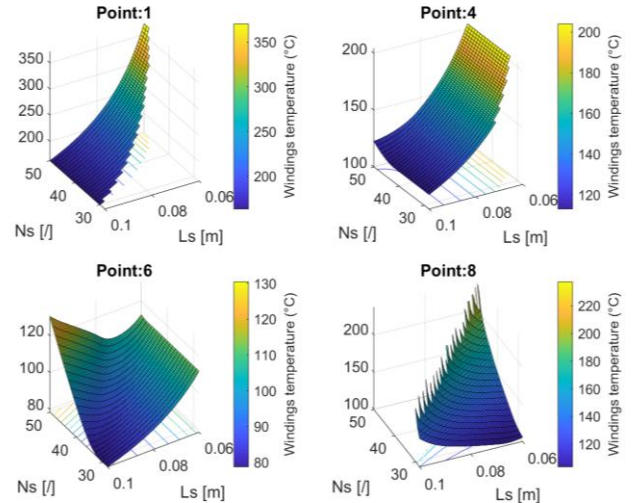


Fig. 5. Achievable areas without the temperature loop and winding temperature evolution $T_j(1)$ for 4 selected operating points.

Fig. 6 shows the evolution of the normalized objective function of the O3 loop as a function of L_s and a discrete variation of N_s . The calculation time to obtain this area was 5 days with a parallel calculation on the 8 operating points. The river shaped possible domain is mainly due to the operating points no. 1 and 8 in this example. Outside this domain, the

constraints of (1) are not respected. In this case, the possible domain might become narrow or non-existent. The normalized objective function has as a reference its minimum value. Thus, the value shows the additional loss ratio in comparison with the minimum. The global minimum among the calculated points is illustrated by a red point on Fig. 6.

The nature of the objective function with a large and undefined area requires an optimization method that is particularly robust and able to find the achievable area. In addition, N_s is a discrete variable (integer) and must be managed by the algorithm. A mesh adaptive direct search (MADS) algorithm for blackbox optimization (NOMAD) [10] is used with a parallel calculation for the 8 operating points starting with an initial unachievable point in the field $L_s = [30, 200] \times 10^{-3}$ m and $N_s = [20, 90]$. The obtained solution is $L_s = 93.7 \times 10^{-3}$ m and $N_s = 31$ turns. The calculation time was around 15 h.

B. With the temperature loop

Adding a temperature loop O1 highly increases the calculation time. In order to get an area that is similar to the Fig. 6 for the same domain and with the same resolution, the calculation time takes 25 days using parallel calculations for the 8 operating points.

With O1 the optimization problem including the 8 previous operating points becomes impossible regarding the technical specifications. Indeed, there is no solution within the defined domain. There no achievable common area (L_s, N_s) between the operating points no. 1 and 8.

Nevertheless, the optimization problem solved for 7 operating points after excluding the point no. 1 (points from 2 to 8). Fig. 7 shows the evolution of the normalized objective function of the loop O3 as function of L_s and N_s for the domains $L_s = [50, 150] \times 10^{-3}$ m and $N_s = [20, 60]$. The achievable area on Fig. 7 becomes wider than that of Fig. 6. The global minimum among the calculated points is stamped by a red point. The obtained solution is $(L_s, N_s)^* = (108 \times 10^{-3} \text{ m}, 20)$ for a calculation time of about 3 days.

V. CONCLUSION

This article presents an advanced layered multi-physical semi-analytical model of IPMSM for EV traction application intended to sizing optimization. A typical design problem applied to a traction machine on several operating points is presented. The analysis of the optimization problem is made from the achievable areas evolution of the temperatures and the objective function for different cases. The optimal solutions obtained by MADS algorithm for blackbox optimization (NOMAD) are given with the magnitude of the computation time.

ACKNOWLEDGMENT

This work was supported by RENAULT-SAS, Guyancourt France. This scientific study is related to the project "Conception optimale des chaines de Traction Electrique" (COCTEL) financed by the "Agence De l'Environnement et de la Maîtrise de l'Énergie" (ADEME).

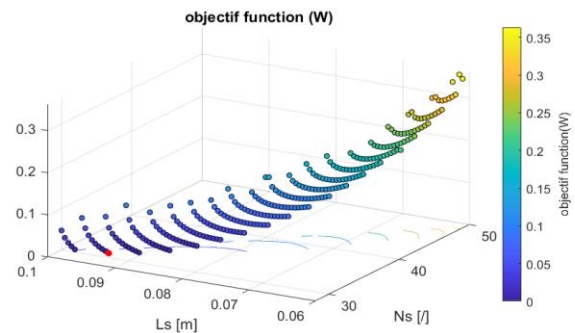


Fig. 6. Evolution of the normalized objective function of the O3 loop as a function of L_s , and of a discrete variation of N_s .

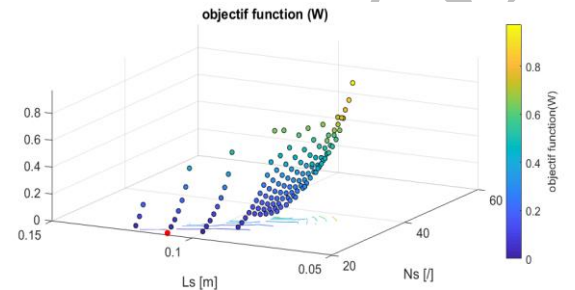


Fig. 7. Evolution of the normalized objective function of the loop O3 in function of L_s , and of a discrete variation of N_s for 7 operating points (2-8).

REFERENCES

1. E. Carraro, M. Morandin and N. Bianchi, "Traction PMASR Motor Optimization According to a Given Driving Cycle," in IEEE Transactions on Industry Applications, vol. 52, no. 1, pp. 209-216, Jan.-Feb. 2016, doi: 10.1109/TIA.2015.2477479.
2. W. Han, C. Van Dang, J. Kim, Y. Kim and S. Jung, "Global-Simplex Optimization Algorithm Applied to FEM-Based Optimal Design of Electric Machine," in IEEE Transactions on Magnetics, vol. 53, no. 6, pp. 1-4, June 2017, Art no. 8106904, doi: 10.1109/TMAG.2017.2684184.
3. A. Frias, A. Kedous-Lebouc, C. Chillet, L. Albert, L. Calegari and O. Messal, "Loss Minimization of an Electrical Vehicle Machine Considering Its Control and Iron Losses," in IEEE Transactions on Magnetics, vol. 52, no. 5, pp. 1-4, May 2016, Art no. 8102904, doi: 10.1109/TMAG.2016.2517657.
4. W. Yan *et al.*, "Design and multi-objective optimisation of switched reluctance machine with iron loss," in IET Electric Power Applications, vol. 13, no. 4, pp. 435-444, 4 2019, doi: 10.1049/iet-epa.2018.5699.
5. R. Benlamine, Y. Benmessaoud, F. Dubas and C. Espanet, "Nonlinear Adaptive Magnetic Equivalent Circuit of a Radial-Flux Interior Permanent-Magnet Machine Using Air-Gap Sliding-Line Technic," 2017 IEEE Vehicle Power and Propulsion Conference (VPPC), Belfort, 2017, pp. 1-6.
6. O. Messal, L. Lambourg, F. Dubas, A. Kedous-Lebouc, S. Harmand, C. Chillet, "Multi-Physic Analysis of Electrical Machines: Hybrid Electro-Magneto-Aero-Thermal Modeling", 19th International Conference on Electrical Machines and Systems – ICEMS 2017, 7–8 Jun. 2017, San Francisco, USA.
7. O. Messal, F. Dubas, R. Benlamine, A. Kedous-lebouc, C. Chillet, and C. Espanet, "Iron Losses in Electromagnetic Devices: Nonlinear Adaptive MEC & Dynamic Hysteresis Model," Preprints (MDPI: Energies), Jan. 2017, DOI: 2017010131.
8. C.P. Steinmetz, "On the law of hysteresis," in Proceedings of the IEEE, vol. 72, no. 2, pp. 197-221, Feb. 1984
9. P. Jandaud, L. Lambourg, S. Harmand. "Aero-Thermal Optimization of a Heat Sink using Variable Neighbourhood Search." Journal of Applied Fluid Mechanics, Special Issue 1, vol. 9, pp. 31-37, 2016.
10. Luong, Huong & Messine, Frederic & Henaux, Carole & Bueno Mariani, Guilherme & Voyer, Nicolas & Mollov, Stefan. (2019). Comparison between fmincon and NOMAD optimization codes to design wound rotor synchronous machines. International Journal of Applied Electromagnetics and Mechanics. 60. s1-s14. 10.3233/JAE-191108.